

1 **A multi-model approach to evaluating target phosphorus loads for Lake Erie**

2

3 Donald Scavia^{a,*}, Joseph V. DePinto^b, Isabella Bertani^a

4

5 ^a Water Center, Graham Sustainability Institute, University of Michigan, 625 East Liberty Road,
6 Ann Arbor, MI 48193, USA

7 ^b LimnoTech, 501 Avis Drive, Ann Arbor, MI 48108, USA

8

9

10

11 * Corresponding author: scavia@umich.edu

12

13
14
15
16
17
18
19
20
21
22
23
24
25
26
27
28
29
30
31
32
33
34

ABSTRACT

In response to water quality changes in the Great Lakes since implementing the 1978 Amendment to the Great Lakes Water Quality Agreement, the US and Canada renegotiated the agreement in 2012, requiring the governments to review and revise phosphorus (P) load targets, starting with Lake Erie. In response, the governments supported a multi-model team to evaluate the existing objectives and P load targets for Lake Erie and provide the information needed to update those targets. Herein, we describe the process and resulting advice provided to the binational process. The collective modeling effort concluded that avoiding severe Western Basin (WB) cyanobacteria blooms requires: 1) focusing on reducing total P loading from the Maumee River, with an emphasis on high-flow events during March – July, 2) focusing on dissolved reactive P load alone will not be sufficient because there is significant bioavailable P in the particulate phosphorus portion of the load, and 3) loading from the Detroit River is not a driver of cyanobacteria blooms. Reducing Central Basin (CB) hypoxia requires a CB+WB load reduction greater than what is needed to reach the WB cyanobacteria biomass goal. Achieving *Cladophora* thresholds will be challenging without site-specific load reductions, and more research is needed. .

Keywords: Loading targets, Great Lakes Water Quality Agreement, Lake Erie, Eutrophication Models

35 **Introduction**

36 In response to significant water quality changes in the Great Lakes since implementing the 1978
37 Amendment to the Great Lakes Water Quality Agreement (GLWQA) (e.g., Evans et al., 2011;
38 IJC, 2014; Scavia et al., 2014), the US and Canada renegotiated the GLWQA (GLWQA, 2012).
39 Annex 4 of the 2012 GLWQA Protocol set interim phosphorus (P) loading targets identical to
40 those established in the 1978 Amendment, and required the US and Canadian governments to
41 review those targets and recommend adjustments if needed, starting with Lake Erie.

42 As part of the GLWQA review, a committee of modelers examined data and models used to
43 support the P target loads in the 1978 Amendment relative to the current status of the Lakes and
44 models (DePinto et al., 2006). At that time, a set of Great Lakes eutrophication models were used
45 to help establish target P loads designed to eliminate excess algae growth and to reduce areas of
46 low dissolved oxygen (DO) concentration – key eutrophication symptoms at that time. Those
47 models ranged from simple empirical relationships to kinetically complex, process-oriented
48 models (Bierman, 1980; Vallentyne and Thomas, 1978), and post-audit of several of those
49 models confirmed they had established sound relationships between P loading and system-wide
50 averaged P and chlorophyll-*a* concentrations (e.g., DiToro et al., 1987; Lesht et al., 1991).

51 However, DePinto et al. (2006) concluded that those models were not resolved enough spatially
52 to capture the characteristics of nearshore eutrophication, nor the impacts of more recent
53 ecosystem changes, such as impacts from dreissenid mussels and other invasive species. Nor
54 were they designed to address harmful algal blooms (HABs). Their recommendation was to
55 establish a new effort to quantify relative contributions of the factors controlling Great Lakes re-
56 eutrophication (Scavia et al., 2014), and to revise quantitative relationships among those
57 stressors and eutrophication indicators such as HABs, hypoxia, and nuisance benthic algae.

58 In response, several new Great Lakes modeling efforts were initiated, and given the availability
59 of these new models, the parties to the GLWQA, Environment Canada and the US EPA,
60 supported a new team to evaluate the interim P objectives and load targets for Lake Erie and to
61 provide the information needed to update those targets. Herein, we describe that process and the
62 resulting advice provided to the GLWQA process because the Lake Erie plan is intended to also
63 serve as a template for the other Great Lakes.

64 **Approach**

65 *Ecosystem Response Indicators* – Before initiating the modeling work, Ecosystem Response
66 Indicators (ERIs) and their associated metrics were established with the GLWQA Annex 4
67 Nutrient Objectives and Targets Task Team (GLWQA, 2015). Four ERIs of Lake Erie
68 eutrophication appropriate for the Annex 4 Objectives were selected:

- 69 • *Western Basin (WB) cyanobacteria biomass* represented by the maximum 30-day average
70 cyanobacteria biomass
- 71 • *Central Basin (CB) hypoxia* represented by number of hypoxic days; average extent of
72 hypoxic area during summer; and average hypolimnion DO concentration during August
73 and September
- 74 • *Basin-specific overall phytoplankton biomass* represented by summer average
75 chlorophyll-*a* concentration
- 76 • *Eastern Basin (EB) Cladophora* represented by dry weight biomass and stored P content.

77 *Multi-Model Strategy* – A multi-model approach was used to explore relationships between the
78 ERIs and P loads because a suite of models with a broad range of complexities and approaches

79 affords an informative comparison of results. Bierman and Scavia (2013) and Weller et al.
80 (2013) identified a number of benefits of applying multiple models of differing complexity:

- 81 • Problems and data are viewed from different conceptual and operational perspectives
- 82 • The level of risk in environmental management decisions is reduced
- 83 • Model diversity adds more value to the decision process than model multiplicity
- 84 • Findings are stronger when multiple lines of evidence are available
- 85 • Using multiple models increases knowledge and understanding of underlying processes
- 86 • Average predictions from a set of models are typically better than from a single model
- 87 • Information from multiple models can help quantify uncertainty
- 88 • Multiple models can expand opportunities for additional stakeholders to participate
- 89 • Reconciling differences among models provides insights on key sources and processes

90 There is also precedent for using multi-model approaches to support management decisions. As
91 noted above, this approach was used in the late 1970's to establish the original target P loads for
92 the Great Lakes (Bierman, 1980). In that case, the six models ranged in complexity from an
93 empirical steady state model (Vollenweider, 1976) to more complex, mechanistic models of
94 Lake Erie (Di Toro and Connolly, 1980) and Saginaw Bay (Bierman and Dolan, 1981).

95 Additional examples include addressing polychlorinated biphenyls (PCBs) in Lake Ontario (IJC,
96 1988), and nutrient loads for the Neuse River Estuary (Stow et al., 2003), the Gulf of Mexico
97 (Scavia et al., 2004), and the Chesapeake Bay (Weller et al., 2013).

98 After establishing the ERIs, model equations, coefficients, driving variables, assumptions, and
99 time step of predictions were described; calibrations, confirmations, and
100 uncertainties/sensitivities were compared; and the ability of each model to develop ERI metric

101 load-response curves were reviewed. With this information and results from previous
102 publications, the model capabilities were reviewed with respect to the following evaluation
103 criteria:

- 104 • *Applicability to ERI metrics:* The models' ability to address the spatial, temporal, and
105 kinetic characteristics of the ERI metrics. While models that address other objectives can
106 be informative, highest priority was given to those that can address the ERIs directly.
- 107 • *Extent/quality of calibration and confirmation:* Calibration – The models' ability to
108 reproduce ERI metric state-variables and internal processes. Post-calibration testing –
109 The models' ability to replicate conditions not represented in the calibration data set.
- 110 • *Extent of model documentation:* The extent of documentation, including descriptions of
111 model kinetics calculations, inputs, calibration, confirmation, and applications.
- 112 • *Level of uncertainty analysis:* The extent to which the models evaluated uncertainty and
113 sensitivity, including for example, those associated with measurement error, model
114 structure, parameterization, aggregation, and uncertainty in characterizing natural
115 variability.

116 ***The Models*** - The models that satisfied these criteria are summarized in Table 1 and described
117 briefly below. Model formulation, calibration, confirmation, and sensitivity/uncertainty, as well
118 as the construction of load-response curves are provided in more detail in Scavia et al. 2016 and
119 in this issue (Bertani et al., this issue; Bocaniov et al., this issue; Chapra et al., this issue;
120 Rucinski et al., this issue; Stumpf et al., this issue; Valipour et al, this issue; Verhamme et al., this
121 issue; Zhang et al., this issue), and in Auer et al. (2010), Canale and Auer (1982), Tomlinson et
122 al. (2010) and Lam et al. (2008, 1987, 1983).

123 *Total Phosphorus Mass Balance Model* (Chapra et al., this issue) – The original version of this
124 parsimonious total phosphorus (TP) mass balance model was used (along with other models) to
125 establish P loading targets for the 1978 Great Lakes Water Quality Agreement. The model has
126 been subsequently revised and updated, including the expansion of the calibration dataset
127 through 2010 and an increase in the post-1990 apparent TP settling velocity to improve model
128 performance, suggesting that mussel invasion may have enhanced the lakes’ ability to retain P
129 (Chapra and Dolan, 2012). The model predicts annual average TP concentrations in the offshore
130 waters of the Great Lakes as a function of external load. For Lake Erie, the model computes
131 basin-wide annual average TP concentrations as a function of loads to each basin. In this
132 application, an empirical relationship between summer chlorophyll and TP concentrations
133 derived for each basin was used to predict basin-specific average chlorophyll levels under
134 different TP load scenarios.

135 *U-M/GLERL Western Lake Erie HAB Model* (Bertani et al., this issue) – A probabilistic
136 empirical model developed by Obenour et al. (2014) relates peak summer cyanobacteria biomass
137 in the WB to spring P loading from the Maumee River. The model is calibrated to multiple sets
138 of *in situ* and remotely sensed bloom observations through a Bayesian hierarchical approach that
139 allows for rigorous uncertainty quantification. The model includes a temporal trend component
140 that suggests an apparent increased susceptibility to cyanobacteria blooms over time. For this
141 application, the original model (Obenour et al., 2014) was modified to include an empirical
142 estimate of the bioavailable portion of the TP load as bloom predictor.

143 *NOAA Western Lake Erie HAB Model* (Stumpf et al., this issue) - This model is based on an
144 empirical regression between spring P load or flow from the Maumee River and peak summer
145 cyanobacteria biomass in the WB as determined through satellite imagery (Stumpf et al., 2012).

146 For this application, the model has been modified to account for the potential difference in
147 cyanobacteria response to load intensity in warm vs. relatively cold early summers. An estimate
148 of bioavailable P load was also tested as bloom predictor.

149 *Nine-Box Model* (Lam et al., 2008, 1987, 1983) - This coarse grid (9-box) P mass balance model
150 was developed to quantify the main physical and biochemical processes that influence Lake Erie
151 eutrophication and related hypoxia (Lam et al., 1983). The model was previously calibrated and
152 validated with water quality observations from 1967-1982 (Lam et al., 1987). For this
153 application, the original calibration was modified to account for changes in settling and re-
154 suspension processes due to dreissenid mussel invasion as described in Scavia et al. 2016.

155 *1-Dimensional Central Basin Hypoxia Model* (Rucinski et al., this issue) - A one-dimensional
156 linked vertical hydrodynamic and eutrophication model was previously developed, calibrated,
157 and corroborated with water quality observations in the CB (Rucinski et al., 2014, 2010). The
158 model is driven by a 1-D hydrodynamic model that provides temperature and vertical mixing
159 profiles. The biological portion of the model incorporates P and carbon (C) loading and internal
160 cycling, algal growth and decay, zooplankton grazing, water column oxygen consumption and
161 production processes, and sediment oxygen demand (SOD). The model has been tested with 19
162 years (1987-2005) of observed loading rates and meteorological conditions to understand the
163 relative contribution of stratification conditions versus P loading extent and seasonal timing on
164 the severity of hypoxia in the CB.

165 *Ecological Model of Lake Erie - EcoLE* (Zhang et al., this issue) - A two-dimensional
166 hydrodynamic and water quality model based on the CE-QUAL-W2 framework was developed
167 and applied to Lake Erie (Zhang et al., 2008). The model was calibrated with observations from
168 1997 and verified with data collected in 1998 and 1999. The model has been used to estimate

169 the impact of grazing and nutrient excretion by dreissenid mussels on phytoplankton biomass
170 and seasonal succession (Zhang et al., 2011). As part of this application, the model was also used
171 to estimate the spatial distribution and relative contribution of different external and internal P
172 sources to the overall P lake budget.

173 *Western Lake Erie Ecosystem Model - WLEEM* (Verhamme et al., this issue) - The Western Lake
174 Erie Ecosystem Model (WLEEM) is a three-dimensional, fine-scale, process-based, linked
175 hydrodynamic-sediment transport-eutrophication model developed to simulate water quality
176 responses to changes in meteorological conditions and loads of water, sediments, and nutrients to
177 the WB. The numerous state variables encompass three phytoplankton groups, including
178 cyanobacteria. In this application, the model was used to simulate the response of WB summer
179 cyanobacteria biomass to a broad suite of P load scenarios, including assessing the impact of
180 potential load reduction strategies selectively targeting specific tributaries or specific P forms
181 (dissolved reactive P (DRP) vs. TP).

182 *ELCOM-CAEDYM* (Bocaniov et al., this issue) – This is a three-dimensional hydrodynamic and
183 ecological model that dynamically couples a hydrodynamic model (Hodges et al., 2000) with a
184 bio-geochemical model (Hipsey, 2008). The model was calibrated and applied to Lake Erie to
185 explore the effect of mussel grazing on phytoplankton biomass, the sensitivity of thermal
186 structure to variations in meteorological parameters, the effects of winter ice on water quality
187 parameters, and the variability in hypoxic area extent as a function of bottom water DO
188 concentration (Bocaniov and Scavia, 2016; Bocaniov et al., 2014; Leon et al., 2011; Liu et al.,
189 2014; Oveisy et al., 2014). As part of this application, different DO concentration thresholds (1-4
190 mg/L) were used for defining hypoxia when comparing P loading scenarios.

191 *Eastern Basin Cladophora modeling* – The Annex 4 multi-model work for this ERI was
192 conducted using the Great Lakes *Cladophora* Model (Auer et al. 2010). This model simulates
193 biological processes driving *Cladophora* biomass and stored P, and it predicts *Cladophora*
194 standing crop as a function of depth, light, temperature, and DRP concentration. The model was
195 originally calibrated and verified with data from Lake Huron and Lake Michigan (Tomlinson et
196 al., 2010). For the Annex 4 analysis, the model was applied to Lake Erie’s EB (see Scavia et al.
197 2016); and results relating *Cladophora* biomass to in-lake DRP concentrations were linked to
198 output from the Total Phosphorus Mass Balance Model and an empirical relationship between
199 TP and DRP concentrations (Chapra et al., this issue). Because of the insufficient time,
200 resources, and data available in the time frame of the Annex 4 work plan, it was recognized that
201 this generic application was a preliminary estimate and that additional site-specific research,
202 monitoring, and modeling would be needed to obtain a more confident estimate of target P loads
203 for the Eastern Basin. In response, following the Annex 4 work, Valipour et al. (this issue) linked
204 the *Cladophora* Growth Model (GCM) (Higgins, et. al., 2006) with a high-resolution 3-D
205 hydrodynamic and water quality model (ELCOM-CAEDYM) to evaluate the fine-scale response
206 of *Cladophora* biomass along the northern shoreline of the EB to changes in external phosphorus
207 loads. While results from this work were not available at the time the original multi-model effort,
208 they provide relevant new insight on the relative contribution of local tributary loads vs.
209 offshore-nearshore nutrient exchanges to *Cladophora* growth in the EB of Lake Erie.

210 *Phosphorus Loadings and Scenarios* – All of the models include P loading as input, and used
211 2008 loads and conditions as baselines for comparison. Maccoux et al. (this issue) provides a
212 detailed long-term analysis of TP (1967-2013) and DRP (2009-2013) loads delivered annually to
213 Lake Erie. The analysis confirms that after a period of gradual decline in the 70s and early 80s,

214 TP loads have shown high year-to-year variation, but no clear long-term trend. Inter-annual
215 variability is largely driven by hydrometeorological conditions, which modulate the timing and
216 magnitude of surface runoff and ultimately the amount of nutrients delivered to the lake (Dolan
217 and Richards, 2008). During 2003-2013, TP from non-point sources contributed on average 71%
218 of the total annual load, while point sources accounted for 19% and atmospheric load and inputs
219 from Lake Huron made up the remaining 10%. TP loads differ substantially among basins, with
220 the WB receiving on average 60% of the whole lake load, and the CB and EB receiving 28% and
221 12%, respectively. For 2003-2013, annual loads to the three basins ranged between 487-1854
222 metric tons (MT) in the EB (average: 1059 MT), 1411-3703 MT in the CB (average: 2551 MT),
223 and 3941-7080 MT in the WB (average: 5493 MT).

224 DRP represented on average 30% of the TP load during 2009-2013, with the WB receiving on
225 average 66% of the whole lake DRP load and the CB and EB receiving approximately 26% and
226 9%, respectively. Non-point and point sources contributed on average 49% and 39% of the total
227 annual DRP load, respectively, with atmospheric sources and loads from Lake Huron making up
228 the remaining 12%.

229 The large TP and DRP loads delivered to the WB derive overwhelmingly from two major
230 sources: the Maumee and Detroit rivers. The vast majority of the P delivered by the Maumee
231 River originates from agricultural sources (Han et al., 2012), which dominate the watershed, and
232 are the primary cause of the extremely high TP concentrations in the Maumee (and other WB
233 tributaries) compared to the Detroit River (Fig. 1). As shown in Fig. 1, the Detroit River P
234 concentration is well below that required for producing a cyanobacteria bloom.

235 While agricultural non-point sources are also primarily responsible for high DRP concentrations
236 in the Maumee, point source contributions result in relatively large DRP loads in the Detroit

237 River as well (Maccoux et al., this issue). As a consequence, while the Maumee River
238 contributes only about 5% of the total flow into the WB, it contributes approximately 48% of the
239 TP load and 31% of the DRP load. On the other hand the Detroit River contributes 41% and
240 59% of the TP and DRP load, respectively, despite accounting for over 90% of the flow (IJC,
241 2014; Maccoux et al., this issue).

242 A recent long-term (1975-2013) analysis of the Maumee River discharge and nutrient loads
243 showed that while TP concentrations remained stable since the 1990s, DRP concentrations have
244 increased (Stow et al., 2015). However, the authors also show that both TP and DRP loads have
245 increased since the 1990s as a result of a concurrent increase in river discharge. The analysis also
246 suggests the occurrence of changes in load seasonality over the past two decades, with a gradual
247 increase in March discharge and P loads. This is especially important as both TP and DRP loads
248 tend to peak in March while typically showing relatively low values from July to October (Stow
249 et al., 2015).

250 Long-term and seasonal changes in the Maumee DRP loads have received increased attention as
251 DRP is generally assumed to be readily available to algae (e.g., Baker et al., 2014). Several algal
252 bioavailability assays conducted in the Maumee River have confirmed that while DRP is
253 virtually 100% bioavailable to algae, the other major fraction of the P load – particulate
254 phosphorus (PP) – is only partially available (DePinto et al., 1981; Young et al., 1985). Results
255 from algal assays were generally consistent with chemical fractionation studies in indicating that
256 approximately 20-40% of the Maumee PP load is bioavailable (see review in Bertani et al., this
257 issue). Wherever possible, the models included in this effort accounted for the different
258 bioavailability of DRP and PP, either by explicitly incorporating processes contributing to in-
259 lake cycling (e.g., Bocaniov et al., this issue; Rucinski et al., this issue; Verhamme et al., this

260 issue; Zhang et al., this issue) or by using the best available knowledge to provide an estimate of
261 the bioavailable fraction of the P load (Bertani et al., this issue; Stumpf et al., this issue).
262 However, the load-response curves estimated by each model are expressed in terms of TP, the
263 component currently measured by most monitoring programs and directly addressed by the
264 GLWQA Nutrient Annex. In developing loading scenarios, 2008 was chosen as a baseline year
265 because its load was closest to the original 1978 Annex 3 target of 11,000 MT. At least six load
266 scenarios, defined as 0%, 25%, 50%, 75%, 100%, and 125% of the 2008 TP load, were used to
267 build load-response curves. In some cases, DRP load reductions were also evaluated.

268 **Results and Discussion**

269 *Load-response curves*

270 *Western Basin cyanobacteria summer biomass* - The three models used to generate HAB
271 response curves identified P load from the Maumee River as the main driver of bloom size, with
272 relatively similar critical load periods across models (mid-February-June for the Bayesian model;
273 March-July for the other two models) (Fig. 2).

274 A peak 30-day average cyanobacteria biomass threshold of 9600 MT was selected to provide an
275 illustrative comparison of the effectiveness of load reductions (Table 2). This threshold was
276 chosen because most blooms perceived as “severe” since the early 2000s had satellite-estimated
277 peak 30-day mean bloom sizes > 9600 MT.

278 Differences in model inputs and outputs need to be taken in consideration when comparing
279 response curves. Because the models considered somewhat different loading periods, to facilitate
280 comparisons, spring load is expressed in the response curves as average monthly load (Fig. 2). In
281 addition, the models used different methods to determine peak 30-day average cyanobacteria

282 biomass. The satellite-derived estimates of maximum 30-day average bloom size used by the
283 empirical models are calculated from consecutive 10-day composite images, which are in turn
284 obtained by summing the highest biomass values observed at each pixel over each 10-day period
285 (Stumpf et al., 2012). WLEEM, on the other hand, simulates daily average basin-wide
286 cyanobacteria biomass, from which the maximum 30-day moving average is calculated
287 (Verhamme et al., this issue). As a result, a satellite-derived bloom size of 9600 MT corresponds
288 to a lower WLEEM-computed bloom size. To account for this, an adjustment was made to
289 convert the satellite-derived threshold of 9600 MT (Fig. 2a-b) to a “WLEEM equivalent” of
290 7830 MT (Fig. 2c) (Verhamme et al., this issue).

291 The load-response curves indicate that spring Maumee River TP load reductions below 180
292 MT/month (Stumpf et al., this issue), 178 MT/month (Verhamme et al., this issue), and 230
293 MT/month (under 2008 conditions; Bertani et al., this issue) result in a mean bloom size below
294 the selected threshold. These monthly loads correspond to cumulative Maumee March-July loads
295 of 890-1150 MT (mean \pm st. dev. = 980 ± 147 MT) and to cumulative Maumee annual loads of
296 1679-2170 MT (mean \pm st. dev. = 1849 ± 278 MT) (Table 2).

297 The models generally agree that both the DRP and PP fractions of the TP load need to be taken
298 into consideration when setting HAB-related load targets and that management strategies
299 focused only on DRP will not likely be sufficient to achieve target bloom sizes (Bertani et al.,
300 this issue; Verhamme et al., this issue). WLEEM also underscores the focus on the Maumee
301 watershed when setting HAB-related load targets (Verhamme et al., this issue). Response curves
302 obtained by reducing the Maumee load vs. reducing loads from all WB tributaries are very
303 similar, indicating that load reduction from the Maumee River is by far the most important. Their
304 evaluation of HAB response to Detroit River TP load reductions confirms the negligible role that

305 the Detroit River plays in bloom formation, although loads from the Detroit River do influence
306 other ecosystem properties such as TP, DRP, and total chlorophyll levels in the WB (Verhamme
307 et al., this issue), and CB hypoxia (see “Central Basin Hypoxia” section).

308 *Basin-specific overall phytoplankton biomass* – A recent long-term analysis of the trophic state
309 of the Great Lakes showed that average summer chlorophyll-*a* concentrations in the CB and EB
310 of Lake Erie rarely exceeded 2.5 µg/L over the past three decades (Dove and Chapra, 2015),
311 indicating that further decreases in summer phytoplankton biomass in these two basins are not
312 needed (Scavia et al. 2016). Load-response curves for total chlorophyll are therefore only
313 presented for the WB, the most productive of the three basins (Dove and Chapra, 2015). An
314 analysis of the basin-specific TP concentrations predicted by the Total Phosphorus Mass Balance
315 model suggested that a 40% reduction from the 2008 WB and CB loads would result in a 25-
316 30% decrease in average spring TP concentrations in each basin (Chapra et al., this issue;
317 GLWQA, 2015), thereby most likely preventing significant impacts on the basins` carrying
318 capacity and fish productivity (GLWQA, 2015; Scavia et al. 2016s).

319 Based on analysis of model performance, four models were judged suitable for exploring the
320 relationship between WB total phytoplankton biomass and external TP loading (Fig. 3). Direct
321 comparisons across load-response curves are difficult because the models used different
322 averaging periods for reporting summer mean chlorophyll-*a* concentrations (Scavia et al. 2016).
323 To facilitate comparisons, chlorophyll concentrations from each model were converted to a
324 percent of the chlorophyll value estimated for the highest load. All response curves were plotted
325 as a function of WB loads (Fig. 3) because CB and EB loads have negligible influence on
326 phytoplankton growth in the WB. Whenever whole lake loads were used in the original model

327 application, they were converted to corresponding WB loads based on the ratio of the 2008 WB
328 load to the whole lake load.

329 These models span a broad range of modeling approaches and complexity. For example, Chapra
330 et al. (this issue) compute chlorophyll concentrations by combining a parsimonious TP mass-
331 balance model with a relatively simple empirical relationship between August chlorophyll and
332 in-lake TP concentrations. On the other hand, the ELCOM-CAEDYM, EcoLE, and WLEEM
333 models simulate several complex biophysical processes and multiple ecological drivers in
334 addition to P concentrations when predicting chlorophyll-*a*, and their results are averaged over
335 different summer months (June-August for ELCOM-CAEDYM and EcoLE, and July-September
336 for WLEEM). The broad diversity in model formulation, assumptions, and level of complexity
337 provides insight on the range of expected outcomes (Fig. 3). While no specific objective was
338 established for WB total phytoplankton biomass, it is instructive to note that reducing loads to
339 prevent significant HABs (Table 2) would likely reduce total phytoplankton biomass by ca. 25%
340 in the WB.

341 *Central Basin Hypoxia* – The models used for this ERI were all calibrated and to varying extent
342 confirmed over recent but different time periods, and are therefore good representations of the
343 current state of the system. While most models are vertically resolved into several layers that
344 allow for a fine-scale representation of seasonal variations in DO profiles, the 9-Box model's 2-
345 layer resolution makes comparisons difficult. For this reason, the 9-Box model was not included
346 in the composite recommendations. The hypoxia response curves from each model were plotted
347 as a function of the annual WB + CB TP loads (Fig. 4). When whole lake loads were used in the
348 original model application, they were converted to WB + CB loads based on the ratio of the 2008
349 WB + CB load to the whole lake load.

350 The response curves for August-September average hypolimnetic DO concentration (Fig. 4a)
351 show similar decreasing trends with increasing loads. Some of the differences among models,

352 especially at lower loads, could be partly attributed to the fact that the 1-D model simulates
353 horizontally-averaged DO, while the other models simulate horizontally-resolved DO
354 concentrations in the bottom layer (0.5-1.0 m for ELCOM-CAEDYM; 1.0 and 1-3 m for
355 EcoLE). Differences could also be attributed to different formulations of SOD, which becomes
356 more important at lower external loads. The 1-D model (Rucinski et al., this issue) also
357 compared two different approaches to estimate loads entering the CB from the WB. One method
358 assumed a constant net apparent TP deposition rate previously estimated for the WB, whereas
359 the alternative approach used nutrient loads from the WB to the CB as simulated by WLEEM. A
360 comparison of the respective load-response curves shows that the two methods yield similar
361 results (Fig. 4).

362 There is strong convergence among models at more typical loading rates (Fig. 4a). An example
363 hypolimnetic DO concentration threshold of 4.0 mg/L was selected to compare model
364 predictions because, while hypoxia is typically defined as DO below 2.0 mg/L, Zhou et al. (
365 2013) showed that statistically significant hypoxic areas start to occur when average
366 hypolimnetic water DO concentrations during the summer stratified period are below
367 approximately 4 mg/L. Using that as an example target threshold, model predictions suggest
368 reducing the WB + CB load to below 2600-5100 MT (mean \pm st. dev. = 3840 ± 1001 ; Table 2).

369 The models were also used to relate loads to hypoxic area (area with DO concentration < 2
370 mg/L). ELCOM-CAEDYM estimates this metric directly through its fine-scale 3-D approach;
371 the other two models use the empirical relationship between hypoxic area and bottom-layer DO
372 concentration developed by Zhou et al. (2013). As expected, all models show that hypoxic extent
373 decreases with decreasing TP loads (Fig. 4b), and suggest that decreasing the annual WB + CB
374 TP load to 3415 – 5955 MT (mean \pm st. dev. = 4600 ± 989 MT) is needed to reduce the average

375 hypoxic extent to 2000 km² (Fig. 4b and Table 2), a value typical of the mid-1990s that coincides
376 with a period of recovery of several recreational and commercial fisheries in Lake Erie's WB
377 and CB (Ludsin et al., 2001; Scavia et al., 2014).

378 The models also estimated the influence of load reductions on the number of hypoxic days
379 (number of days when average bottom water DO is < 2 mg/L) (Fig. 4c). The models indicate that
380 a WB + CB TP load below 3415-5955 MT/year would result in a decrease in the number of
381 hypoxic days to between 9 and 42 (Fig. 4c).

382 The 1-D model simulated hypoxia response to load reductions under the broad range of
383 meteorological conditions observed between 1987 and 2005 (Rucinski et al., this issue). Results
384 indicate that the response to load reductions may show substantial inter-annual variability due to
385 meteorological forces driving mixing regimes. These findings are especially relevant in view of
386 projected changes in future climate conditions, which could result in substantial deviations in the
387 lake's behavior from average model predictions. This uncertainty calls for an adaptive
388 management approach, where the system's response to load reductions is assessed over time and
389 new knowledge is used to regularly update models and management strategies. Rucinski et al. (
390 this issue, 2014) also showed that variations in the lake's thermal structure produced far more
391 inter-annual variability in hypoxic area than variations in the timing, or seasonality, of the load.

392 *Eastern Basin Cladophora* – For this ERI, the Great Lakes *Cladophora* Model (Canale and Auer,
393 1982; Tomlinson et al., 2010) met the criteria required for inclusion in this effort; and while
394 initial results were not used for setting loading targets (see below), it did provide a preliminary
395 estimate. Subsequently, additional site-specific modeling efforts have begun for this portion of
396 the lake, and one of them, a three dimensional hydrodynamic-water quality model by Valipour et
397 al. (this issue) is presented in this special series.

398 For Annex 4 work (See Scavia et al. 2016), the Great Lakes *Cladophora* model relating algal
399 biomass to EB DRP concentrations, , an empirical model relating DRP to TP concentrations
400 (Dove and Chapra, 2015), and the Total Phosphorus Mass Balance Model (Chapra et al., this
401 issue) relating TP concentrations to external TP loads were combined to generate a *Cladophora*
402 biomass-TP load-response curve. Since there is currently no regulatory guidance on acceptable
403 levels of *Cladophora* biomass, a biomass of 30 g dry weight (DW)/m² was suggested as a
404 threshold likely to prevent nuisance conditions (Scavia et al. 2016), and that corresponds to DRP
405 and TP concentrations of 0.9 µg P/L and 6.3 µg P/L, respectively, or a whole-lake TP load below
406 7000 MT/Year. It is important to note that this combined modeling approach was used because
407 of time, resource, and data limitations and it is not site-specific, but rather relates *Cladophora*
408 biomass along the entire north shoreline of the EB to average offshore nutrient concentrations.
409 However, *Cladophora* proliferates in the nearshore, where it is often subjected to direct impacts
410 of point-source and tributary inputs. Nutrient concentrations in the nearshore waters may
411 therefore be higher and more variable than those in the offshore, and as offshore DRP
412 concentrations are reduced, control of *Cladophora* growth is expected to shift toward nearshore
413 inputs, requiring spatially explicit models.

414 Some of these limitations were recently addressed by Valipour et al., this issue. Their 3-D model
415 simulated the predominant physical processes within the *Cladophora* habitat zone (0–8 m depth)
416 in the EB of Lake Erie, with a focus on the northern coast in the vicinity of the Grand River
417 where *Cladophora* is abundant. Model output was input to the Higgins *Cladophora* Growth
418 Model (CGM) (Higgins et. al., 2006) to relate nearshore *Cladophora* biomass to external
419 phosphorus loads. Results showed that while P load reductions can be expected to reduce
420 *Cladophora* biomass in the EB, achieving proposed biomass thresholds may be more challenging

421 than previously thought (Fig. 5). Coastal upwelling events often input significant nutrients along
422 much of the north shore, particularly during May and June when conditions are optimal for
423 *Cladophora* growth. Simulations confirmed that P supplies from both the offshore and local
424 sources (e.g. the Grand River) are capable of generating biomass above the proposed threshold in
425 the vicinity of the Grand River. The relative importance of offshore-nearshore nutrient
426 exchanges vs. local tributary inputs in driving nearshore P concentrations and *Cladophora*
427 growth varies within and across years, most likely resulting in substantial variability in
428 *Cladophora* response as whole lake loads are reduced. Generally, these results indicate that
429 measures aimed at decreasing *Cladophora* biomass in the EB of Lake Erie should take into
430 account nutrient sources from both the offshore region and local tributary inputs (Valipour et al.,
431 this issue). These results also point to a need for an Adaptive Management plan for Eastern
432 Basin *Cladophora* that includes research, monitoring, and modeling.

433

434 ***Benefits of the multi-model approach and future research needs***

435 Although the models vary substantially in formulations, assumptions, and parameterizations, the
436 load-response curves generally showed considerable agreement, providing confidence in the
437 robustness of the recommendations. However, quantifying each model's uncertainty explicitly
438 would have further enhanced confidence (Kim et al., 2014). While such quantification is easily
439 accommodated in some models, it is much more difficult, if even possible, for others. The HAB
440 models provide an example. They range from a parsimonious empirical Bayesian hierarchical
441 model capable of accounting quantitatively for model error, bloom measurement error, and
442 uncertainty in parameter estimates to a complex process-based deterministic model that provides
443 model uncertainty in terms of quantitative comparisons of simulations and field observations for

444 all years simulated, but is too complex and runtime consuming for a full Monte Carlo uncertainty
445 analysis. While this illustrates a trade-off between providing causal understanding of ecosystem
446 behavior and rigorously quantifying uncertainty, it also highlights one of the benefits of the
447 multi-model approach. In that approach, the range of predicted outcomes illustrates the degree
448 of confidence in our understanding of, and the predictability of, the system's response to loads.
449 The thorough representation of uncertainty possible with the statistical models also helps identify
450 key scientific gaps limiting our predictive understanding of the system's behavior and can guide
451 future experimental and monitoring efforts. For example, including multiple independent sets of
452 bloom observations in the Bayesian model suggests that uncertainty associated with bloom
453 characterization represents a considerable portion of overall HAB predictive uncertainty (Bertani
454 et al., this issue). More generally, the relatively large uncertainty in HAB predictions highlights
455 once again the need for adaptive management approaches that track the effectiveness of actions
456 and routinely revise models and management decisions based on new information – a point also
457 emphasized in the analysis of variability associated with meteorology in the 1D hypoxia model
458 (Rucinski et al., this issue).

459 In the case of hypoxia, a key source of uncertainty is quantifying the impact of changes in
460 external loads on SOD. Previous studies have shown that SOD represents a substantial portion of
461 total hypolimnetic oxygen demand in the CB (Rucinski et al., 2014), and both SOD and water
462 column oxygen demand are affected by external loads. The hypoxia models used similar
463 approaches to approximate the potential effects of changes in nutrient loads on future SOD.
464 Rucinski et al. (this issue) coupled a relationship between SOD and organic carbon
465 sedimentation rates (Borsuk et al., 2001) with a relationship between P loading and carbon
466 settling from his model to predict future SOD as a function of P loads (Rucinski et al., 2014).

467 Bocaniov et al. (this issue) and Zhang et al. (this issue) used the relationship developed by
468 Rucinski et al. (2014), but allowed for adjustments to temperature and bottom water DO
469 concentrations. These approaches represent our best available estimates of how SOD rates may
470 change as a function of nutrient loads. However, future research should focus on developing
471 long-term measurement and modeling approaches that can improve our understanding of how
472 SOD and benthic nutrient fluxes will change as a result of external load reductions and how
473 accumulation of nutrients and organic matter in the sediments may delay the system's response
474 to load reductions.

475 Valuable insight on critical research gaps can also be gained by exploring discrepancies among
476 the models. For example, comparison of the HAB models suggests that quantifying the
477 contribution of the PP component of the TP load in fueling HABs remains a critical challenge.
478 Numerous studies have quantified the algal availability of PP in the Maumee River (see review
479 in Bertani et al., this issue; DePinto et al., 1981; Young et al., 1985), and this knowledge has
480 been incorporated in all three HAB models through various approaches. However, we still have
481 limited observational knowledge of the ultimate fate of PP as it is delivered to the lake and
482 undergoes processes that influence its bioavailability, including settling, re-suspension, microbial
483 mineralization, and re-cycling by dreissenid mussels and other organisms. Stumpf et al. (this
484 issue) explicitly account for the proportion of the Maumee PP load that is assumed to settle out
485 of the water column before reaching the WB open waters based on a recent field study (Baker et
486 al., 2014b). However, field studies exploring nutrient transport dynamics along the river-lake
487 continuum in western Lake Erie are sparse, and more research is needed to quantify physical
488 processes controlling the ultimate fate of riverine nutrients. The 3-D mechanistic models (e.g.,
489 Bocaniov et al., this issue; Verhamme et al., this issue; Zhang et al., this issue) attempt to

490 explicitly characterize nutrient transport, in-lake dynamics of bioavailable P and kinetic
491 conversions among P forms (e.g., mineralization of organic P to orthophosphate, gradient-driven
492 desorption of orthophosphate from inorganic PP). However, additional measurements of *in situ*
493 biophysical processes in both the water column and sediments that can further constrain the
494 models will help reduce uncertainties.

495 Integrating results from different modeling approaches also allows for exploring processes
496 occurring at different spatio-temporal scales. For example, while the process-based HAB model
497 provides key insight into fine scale bloom spatio-temporal dynamics and underlying
498 mechanisms, the empirical models allow for assessment of system responses at longer time
499 scales. For example, the Bayesian model includes a temporal component that suggests increased
500 susceptibility of western Lake Erie to bloom formation over time, suggesting the same TP load is
501 predicted to trigger a larger bloom under present-day conditions compared to earlier years (Fig.
502 2b). Specifically, the model predicts that under 2008 lake conditions, March-June Maumee TP
503 loads below 230 MT/mo will prevent severe blooms, while under 2014 conditions a TP load of
504 230 MT/month would still result in an average bloom size of 28,000 MT (95% predictive
505 interval: 17,000-38,000 MT) (Fig. 2b). This temporal trend term, estimated by the Bayesian
506 model, remains significantly positive even after accounting for concurrent increases in DRP
507 loads, suggesting that the observed increase in DRP load alone may not be sufficient to explain
508 the apparent enhanced susceptibility. However, results from the other empirical model do not
509 support these findings. They suggest that removing the influence of the July load for relatively
510 cold years prevents under prediction of some of the most recent blooms (Stumpf et al., this
511 issue). Further research is needed to assess whether the lake is becoming more susceptible to
512 bloom formation and, if so, to identify underlying mechanisms, including the role of changes in

513 frequency, magnitude, and timing of extreme weather events (Michalak et al., 2013), the
514 potential impact of selective grazing and nutrient excretion by dreissenid mussels (Arnott and
515 Vanni, 1996; Conroy et al., 2005; Jiang et al., 2015; Vanderploeg et al., 2001; Zhang et al.,
516 2011), the influence of internal loading of both nutrients and cyanobacteria cell inocula (Chaffin
517 et al., 2014b; Rinta-Kanto et al., 2009), the role of nitrogen co-limitation (Chaffin et al., 2014a,
518 2013; Harke et al., 2015), and the influence of changes in the proportion of available vs. non-
519 available fractions of the TP load (Baker et al., 2014a; Kane et al., 2014).

520

521 **Conclusions**

522 The load-response curves presented herein represent our current best estimates of how Lake
523 Erie's ERI metrics will respond to changes in P loads, with the loadings necessary to achieve the
524 example thresholds summarized in Table 2. Results of this multi-model approach suggest:

- 525 • Achieving Western Basin cyanobacteria biomass reduction requires a focus on reducing
526 TP loading from the Maumee River, with an emphasis on high-flow events during March
527 - July. Results suggest that focusing on Maumee DRP load alone will not be sufficient
528 and that P load from the Detroit River is not a driver of cyanobacteria blooms.
- 529 • Reducing Central Basin hypoxia requires a Central + Western Basin annual load
530 reduction greater than what is needed to reach the Western Basin cyanobacteria biomass
531 goal. Load reductions focused on dissolved oxygen concentration and hypoxic areal
532 extent also result in shorter hypoxia duration.
- 533 • While the original Annex 4 analysis indicated that the load reductions suggested for
534 meeting the cyanobacteria and Central Basin hypoxia thresholds would be sufficient to

535 meet the Eastern Basin *Cladophora* biomass goal, more recent work (Valipour, et. al. this
536 issue) does not support this conclusion.

537 These results offered several strategies for setting loading targets under the GLWQA. The
538 thresholds in Table 2 were intended to illustrate the range of load reductions likely needed. They
539 were used by the Objectives and Targets Task Team in their recommendations to the GLWQA
540 Nutrient Annex Subcommittee on loading targets (GLWQA, 2015). Their recommendations, in
541 the context of our findings, were:

- 542 • *Western Basin Cyanobacteria* - To keep blooms below 9600 MT algal dry weight (the
543 size of the blooms observed in 2004 or 2012) 90% of the time, the Task Team
544 recommended a Maumee River March-July TP load of 860 MT and a DRP load of 186
545 MT, consistent with our findings. These loads represent roughly 40% reductions from the
546 2008 spring loads and correspond to Flow Weighted Mean Concentrations (FWMC) of
547 0.23 mg/L TP and 0.05 mg/L DRP. FWMC was included in the Task Team
548 recommendation to address significant inter-annual variability in Maumee River
549 discharge. It is expected that maintaining those concentrations will result in loads below
550 the targets 90% of the time, if climate change does not alter precipitation patterns. It was
551 also noted that, while reducing DRP will have a greater impact than reducing PP,
552 reducing DRP alone will not be sufficient. The Task Team also recommended 40%
553 reductions for all other WB tributaries and the Thames River.

- 554 • *Central Basin Hypoxia* - Our analysis suggested that setting a minimum summer average
555 hypolimnetic DO concentration of 4 mg/L or reducing hypoxia area to less than 2000 km²
556 requires average WB + CB loads of 3840 MT and 4600 MT, respectively (Table 2). The

557 Task Team believed the load reduction to keep summer hypolimnetic DO concentrations
558 at or above 4 mg/L was so restrictive that it might reduce overall productivity and impact
559 fisheries, so they recommended an annual WB + CB TP loading target of 6000 MT,
560 closer to our area-reduction example and expected to maintain summer hypolimnion DO
561 concentrations above 2 mg/L. This load represents a 40% reduction from 2008 WB + CB
562 load levels.

563 • *Eastern Basin Cladophora* - While the original Annex 4 analysis suggests that the
564 cyanobacteria- and hypoxia-driven load targets are sufficient to achieve a desired
565 reduction in *Cladophora* in the EB, the Task Team was not sufficiently confident in the
566 cascade of models used to set a loading target for *Cladophora* (Task Team 2015). They
567 pointed to the need to develop a site-specific model for the north shore of the EB that
568 accounts for nutrient exchanges with the open water, load and transport of specific
569 tributaries, and the role of dreissenids to gain more confidence. A spatially-explicit
570 modeling effort was recently developed to address some of these issues (Valipour et al.,
571 this issue). This work indicates that reducing nearshore *Cladophora* biomass may be
572 more challenging than previously thought, and more research is needed to develop sound
573 recommendations to address *Cladophora* growth in Lake Erie.

574

575 **Acknowledgments**

576 This work was funded in part by the USEPA under contract EP-R5-11-07, Task Order 21 and by
577 the University of Michigan Graham Sustainability Institute.

578

579 **References**

580 Arnott, D.L., Vanni, M.J., 1996. Nitrogen and phosphorus recycling by the zebra mussel
581 (*Dreissena polymorpha*) in the western basin of Lake Erie. *Can. J. Fish. Aquat. Sci.* 53,
582 646–659.

- 583 Auer, M., Tomlinson, L., Higgins, S., Malkin, S., Howell, E., Bootsma, H., 2010. Great Lakes
584 Cladophora in the 21st century: Same alga - different ecosystem. *J. Great Lakes Res.* 36,
585 248–255.
- 586 Baker, D.B., Confesor, R.B., Ewing, D.E., Johnson, L.T., Kramer, J.W., Merryfield, B.J., 2014a.
587 Phosphorus loading to Lake Erie from the Maumee, Sandusky and Cuyahoga rivers: The
588 importance of bioavailability. *J. Great Lakes Res.* 40, 502–517.
- 589 Baker, D.B., Ewing, D.E., Johnson, L.T., Kramer, J.W., Merryfield, B.J., Confesor, R.B.,
590 Richards, R.P., Roerdink, A.A., 2014b. Lagrangian analysis of the transport and processing
591 of agricultural runoff in the lower Maumee River and Maumee Bay. *J. Great Lakes Res.* 40,
592 479–495.
- 593 Bertani, I., Obenour, D.R., Steger, C.E., Stow, C.A., Gronewold, A.D., Scavia, D., n.d.
594 Probabilistically assessing the role of nutrient loading in harmful algal bloom formation in
595 western Lake Erie. *J. Gt. Lakes Res.* This issue.
- 596 Bierman, V., 1980. A Comparison of Models Developed for Phosphorus Management in the
597 Great Lakes, in: Conference on Phosphorus Management Strategies for the Great Lakes. pp.
598 1–38.
- 599 Bierman, V., Scavia, D., 2013. Hypoxia in the Gulf of Mexico: Benefits and Challenges of Using
600 Multiple Models to Inform Management Decisions, in: Presentation at Multiple Models for
601 Management (M3.2) in the Chesapeake Bay. Annapolis, MD.
- 602 Bierman, V.J., Dolan, D.M., 1981. Modeling of Phytoplankton-Nutrient Dynamics in Saginaw
603 Bay, Lake Huron. *J. Great Lakes Res.* 7, 409–439. doi:10.1016/S0380-1330(81)72069-0
- 604 Bocaniov, S., Leon, L., Rao, Y., Schwab, D., Scavia, D., n.d. Simulating the effect of nutrient
605 reduction on hypoxia in central Lake Erie with a three-dimensional lake model. *J. Gt. Lakes*
606 *Res.* This issue.
- 607 Bocaniov, S., Scavia, D., 2016 Temporal and spatial dynamics of large lake hypoxia: Integrating
608 statistical and three-dimensional dynamic models to enhance lake management criteria.
609 *Water Resources Res.* DOI: 10.1002/2015WR018170
- 610 Bocaniov, S., Smith, R., Spillman, C., Hipsey, M., Leon, L., 2014. The nearshore shunt and the
611 decline of the phytoplankton spring bloom in the Laurentian Great Lakes: Insights from a
612 three-dimensional lake model. *Hydrobiologia* 731, 151–172.
- 613 Borsuk, M., Higdon, D., Stow, C., Reckhow, K., 2001. A Bayesian hierarchical model to predict
614 benthic oxygen demand from organic matter loading in estuaries and coastal zones. *Ecol.*
615 *Modell.* 143, 165–181.
- 616 Canale, R., Auer, M., 1982. Ecological studies and mathematical modeling of Cladophora in
617 Lake Huron: 5. Model development and calibration. *J. Great Lakes Res.* 8, 112–125.
- 618 Chaffin, J.D., Bridgeman, T.B., Bade, D.L., 2013. Nitrogen Constrains the Growth of Late
619 Summer Cyanobacterial Blooms in Lake Erie. *Adv. Microbiol.* 16–26.
- 620 Chaffin, J.D., Bridgeman, T.B., Bade, D.L., Mobilian, C.N., 2014a. Summer phytoplankton
621 nutrient limitation in Maumee Bay of Lake Erie during high-flow and low-flow years. *J.*
622 *Great Lakes Res.* 40, 524–531. doi:10.1016/j.jglr.2014.04.009

- 623 Chaffin, J.D., Sigler, V., Bridgeman, T.B., 2014b. Connecting the blooms: Tracking and
624 establishing the origin of the record-breaking Lake Erie *Microcystis* bloom of 2011 using
625 DGGE. *Aquat. Microb. Ecol.* 73, 29–39. doi:10.3354/ame01708
- 626 Chapra, S., Dolan, D., Dove, A., n.d. Mass-balance modeling framework for simulating and
627 managing long-term water quality for the lower Great Lakes. *J. Gt. Lakes Res.* This issue.
- 628 Chapra, S.C., Dolan, D.M., 2012. Great Lakes total phosphorus revisited: 2. Mass balance
629 modeling. *J. Great Lakes Res.* 38, 741–754. doi:10.1016/j.jglr.2012.10.002
- 630 Conroy, J.D., Edwards, W.J., Pontius, R.A., Kane, D.D., Zhang, H., Shea, J.F., Richey, J.N.,
631 Culver, D.A., 2005. Soluble nitrogen and phosphorus excretion of exotic freshwater mussels
632 (*Dreissena* spp.): potential impacts for nutrient remineralisation in western Lake Erie.
633 *Freshw. Biol.* 50, 1146–1162.
- 634 DePinto, J.V., Lam, D., Auer, M.T., Burns, N., Chapra, S.C., Charlton, M.N., Dolan, D.M.,
635 Kreis, R., Howell, T., Scavia, D., 2006. Examination of the status of the goals of Annex 3 of
636 the Great Lakes Water Quality Agreement.
- 637 DePinto, J. V., Young, T.C., Martin, S.C., 1981. Algal-Available Phosphorus in Suspended
638 Sediments from Lower Great Lakes Tributaries. *J. Great Lakes Res.* 7, 311–325.
- 639 Di Toro, D.M., Connolly, J.P., 1980. Mathematical models of water quality in large lakes. Part 2:
640 Lake Erie. EPA-600/3-80-065 Report, Duluth, MN.
- 641 Di Toro, D.M., Thomas, N.A., Herdendorf, C.E., Winfield, R.P., Connolly, J.P., 1987. A post
642 audit of a Lake Erie eutrophication model. *J. Great Lakes Res.* 13, 801–825.
- 643 Dolan, D., Richards, R., 2008. Analysis of late 90s phosphorus loading pulse to Lake Erie, in:
644 Munawar, M., Heath, R. (Eds.), *Checking the Pulse of Lake Erie*. Aquatic Ecosystem
645 Health and Management Society, Burlington, Ontario, pp. 79–96.
- 646 Dove, A., Chapra, S.C., 2015. Long-term trends of nutrients and trophic response variables for
647 the Great Lakes. *Limnol. Oceanogr.* 60, 696–721. doi:10.1002/lno.10055
- 648 Evans, M.A., Fahnenstiel, G., Scavia, D., 2011. Incidental oligotrophication of North American
649 Great Lakes. *Environ. Sci. Technol.* 45, 3297–3303. doi:10.1021/es103892w
- 650 GLWQA, 2015. Recommended Phosphorus Loading Targets for Lake Erie - Annex 4 Objectives
651 and Targets Task Team Final Report to the Nutrients Annex Subcommittee.
- 652 GLWQA, 2012. The 2012 Great Lakes Water Quality Agreement - Annex 4.
653 <http://tinyurl.com/gt92hrh>. Viewed 25 February 2016.
- 654 Han, H., Allan, J., Bosch, N., 2012. Historical pattern of phosphorus loading to Lake Erie
655 watersheds. *J. Great Lakes Res.* 38, 289–298.
- 656 Harke, M.J., Davis, T.W., Watson, S.B., Gobler, C.J., 2015. Nutrient-controlled niche
657 differentiation of western Lake Erie cyanobacterial populations revealed via
658 metatranscriptomic surveys. *Environ. Sci. Technol.* acs.est.5b03931.
659 doi:10.1021/acs.est.5b03931
- 660 Higgins, S.N., Hecky, R.E., Guildford, S.J., 2006. Environmental Controls of *Cladophora*
661 Growth Dynamics in Eastern Lake Erie: Application of the *Cladophora* Growth Model

662 (CGM). *J. Great Lakes Res.* 32, 629–644. doi:10.3394/0380-
663 1330(2006)32[629:ECOCGD]2.0.CO;2

664 Hipsey, M., 2008. The CWR Computational Aquatic Ecosystem Dynamics Model CAEDYM -
665 User Manual. Centre for Water Research, University of Western Australia.

666 Hodges, B., Imberger, J., Saggio, A., Winters, K., 2000. Modeling basin-scale internal waves in
667 a stratified lake. *Limnol. Oceanogr.* 1603-1620.

668 IJC, 2014. A Balanced Diet for Lake Erie: Reducing Phosphorus Loadings and Harmful Algal
669 Blooms. Report of the Lake Erie Ecosystem Priority.

670 IJC, 1988. Report on Modeling the Loading Concentration Relationship for Critical Pollutants in
671 the Great Lakes. IJC Great Lakes Water Quality Board, Toxic Substances Committee, Task
672 Force on Toxic Chemical Loadings.

673 Jiang, L., Xia, M., Ludsin, S.A., Rutherford, E.S., Mason, D.M., Marin Jarrin, J., Pangle, K.L.,
674 2015. Biophysical modeling assessment of the drivers for plankton dynamics in dreissenid-
675 colonized western Lake Erie. *Ecol. Modell.* 308, 18–33.
676 doi:10.1016/j.ecolmodel.2015.04.004

677 Kane, D.D., Conroy, J.D., Peter Richards, R., Baker, D.B., Culver, D.A., 2014. Re-
678 eutrophication of Lake Erie: Correlations between tributary nutrient loads and
679 phytoplankton biomass. *J. Great Lakes Res.* 40, 496–501. doi:10.1016/j.jglr.2014.04.004

680 Kim, D.K., Zhang, W., Watson, S., Arhonditsis, G.B., 2014. A commentary on the modelling of
681 the causal linkages among nutrient loading, harmful algal blooms, and hypoxia patterns in
682 Lake Erie. *J. Great Lakes Res.* 40, 117–129. doi:10.1016/j.jglr.2014.02.014

683 Lam, D., Schertzer, W., Fraser, A., 1987. A post-audit analysis of the NWRI nine-box water
684 quality model for Lake Erie. *J. Great Lakes Res.* 13, 782–800.

685 Lam, D., Schertzer, W., McCrimmon, R., Charlton, M., Millard, S., 2008. Modeling phosphorus
686 and dissolved oxygen conditions pre- and post- Dreissena arrival in Lake Erie, in:
687 Munawar, M., Heath, R. (Eds.), *Checking the Pulse of Lake Erie*. Aquatic Ecosystem
688 Health and Management Society, Burlington, Ontario.

689 Lam, D.C.L., Schertzer, W.M., Fraser, A.S., 1983. Simulation of Lake Erie water quality
690 responses to loading and weather variations. Environment Canada, Scientific series / Inland
691 Waters Directorate; no. 134, Burlington, Ontario.

692 Leon, L.F., Smith, R.E.H., Hipsey, M.R., Bocaniov, S.A., Higgins, S.N., Hecky, R.E.,
693 Antenucci, J.P., Imberger, J.A., Guildford, S.J., 2011. Application of a 3D hydrodynamic-
694 biological model for seasonal and spatial dynamics of water quality and phytoplankton in
695 Lake Erie. *J. Great Lakes Res.* 37, 41–53.

696 Lesht, B.M., Fontaine, T.D., Dolan, D.M., 1991. Great Lakes Total Phosphorus Model: Post
697 Audit and Regionalized Sensitivity Analysis. *J. Great Lakes Res.* 17, 3–17.
698 doi:10.1016/S0380-1330(91)71337-3

699 Liu, W., Bocaniov, S.A., Lamb, K.G., Smith, R.E.H., 2014. Three dimensional modeling of the
700 effects of changes in meteorological forcing on the thermal structure of Lake Erie. *J. Great
701 Lakes Res.* 40, 827–840.

- 702 Ludsin, S., Kershner, M., Blocksom, K., Knight, R., Stein, R., 2001. Life after death in Lake
703 Erie: nutrient controls drive fish species richness, rehabilitation. *Ecol. Appl.* 11, 731–746.
- 704 Maccoux, M., Dove, A., Backus, S., Dolan, D., n.d. Total and soluble reactive phosphorus
705 loadings to Lake Erie. *J. Gt. Lakes Res.* This issue.
- 706 Michalak, A.M., Anderson, E.J., Beletsky, D., Boland, S., Bosch, N.S., Bridgeman, T.B.,
707 Chaffin, J.D., Cho, K., Confesor, R., Daloglu, I., Depinto, J., Evans, M.A., Fahnenstiel,
708 G.L., He, L., Ho, J.C., Jenkins, L., Johengen, T.H., Kuo, K.C., Laporte, E., Liu, X.,
709 McWilliams, M.R., Moore, M.R., Posselt, D.J., Richards, R.P., Scavia, D., Steiner, A.L.,
710 Verhamme, E., Wright, D.M., Zagorski, M.A., 2013. Record-setting algal bloom in Lake
711 Erie caused by agricultural and meteorological trends consistent with expected future
712 conditions. *Proc. Natl. Acad. Sci. U. S. A.* 110, 6448–6452.
- 713 Obenour, D., Gronewold, A., Stow, C.A., Scavia, D., 2014. Using a Bayesian hierarchical model
714 to improve Lake Erie cyanobacteria bloom forecasts. *Water Resour. Res.* 50, 7847–7860.
- 715 Oveysy, A., Rao, Y.R., Leon, L.F., Bocaniov, S.A., 2014. Three-dimensional winter modeling
716 and the effects of ice cover on hydrodynamics, thermal structure and water quality in Lake
717 Erie. *J. Great Lakes Res.* 40, 19–28.
- 718 Rinta-Kanto, J.M., Saxton, M.A., DeBruyn, J.M., Smith, J.L., Marvin, C.H., Krieger, K.A.,
719 Sayler, G.S., Boyer, G.L., Wilhelm, S.W., 2009. The diversity and distribution of toxigenic
720 *Microcystis* spp. in present day and archived pelagic and sediment samples from Lake Erie.
721 *Harmful Algae* 8, 385–394. doi:10.1016/j.hal.2008.08.026
- 722 Rucinski, D., DePinto, J., Beletsky, D., Scavia, D., n.d. Modeling hypoxia in the Central Basin of
723 Lake Erie under potential phosphorus load reduction scenarios. *J. Gt. Lakes Res.* This issue.
- 724 Rucinski, D.K., Beletsky, D., DePinto, J. V., Schwab, D.J., Scavia, D., 2010. A simple 1-
725 dimensional, climate based dissolved oxygen model for the central basin of Lake Erie. *J.*
726 *Great Lakes Res.* 36, 465–476. doi:10.1016/j.jglr.2010.06.002
- 727 Rucinski, D.K., DePinto, J. V., Scavia, D., Beletsky, D., 2014. Modeling Lake Erie’s hypoxia
728 response to nutrient loads and physical variability. *J. Great Lakes Res.* 40, 151–161.
729 doi:10.1016/j.jglr.2014.02.003
- 730 Scavia, D., Allan, J.D., Arend, K.K., Bartell, S., Beletsky, D., Bosch, N.S., Brandt, S.B., Briland,
731 R.D., Daloglu, I., DePinto, J. V., Dolan, D.M., Evans, M.A., Farmer, T.M., Goto, D., Han,
732 H., Höök, T.O., Knight, R., Ludsin, S.A., Mason, D., Michalak, A.M., Richards, R.P.,
733 Roberts, J.J., Rucinski, D.K., Rutherford, E., Schwab, D.J., Sesterhenn, T.M., Zhang, H.,
734 Zhou, Y., 2014. Assessing and addressing the re-eutrophication of Lake Erie: Central basin
735 hypoxia. *J. Great Lakes Res.* 40, 226–246.
- 736 Scavia, D., DePinto, J. V., Auer, M., Bertani, I., Bocaniov, S., Chapra, S., Leon, L., McCrimmon,
737 C., Obenour, D., Rucinski, D., Steger, C., Stumpf, R., Yerubandi, R. Zhang, H., 2016. Great
738 Lakes Water Quality Agreement Nutrient Annex Objectives and Targets Task Team
739 Ensemble Modeling Report. Great Lakes National Program Office, USEPA, Chicago
740 **INSERT URL**
- 741 Scavia, D., Justic, D., Bierman, V., 2004. Reducing Hypoxia in the Gulf of Mexico: Advice from
742 Three Models. *Estuaries* 27, 419–425.

- 743 Stow, C., Roessler, C., Borsuk, M., Bowen, J., Reckhow, K., 2003. Comparison of Estuarine
744 Water Quality Models for Total Maximum Daily Load Development in Neuse River
745 Estuary. *J. Water Resour. Plan. Manag.* 129, 307–314.
- 746 Stow, C.A., Cha, Y., Johnson, L.T., Confesor, R., Richards, R.P., 2015. Long-term and seasonal
747 trend decomposition of Maumee River nutrient inputs to western Lake Erie. *Environ. Sci.*
748 *Technol.* 49, 3392–400. doi:10.1021/es5062648
- 749 Stumpf, R., Johnson, L., Wynne, T., Baker, D., n.d. Forecasting annual cyanobacterial bloom
750 biomass to inform management decisions in Lake Erie. *J. Gt. Lakes Res.* This issue.
- 751 Stumpf, R.P., Wynne, T.T., Baker, D.B., Fahnenstiel, G.L., 2012. Interannual variability of
752 cyanobacterial blooms in Lake Erie. *PLoS One* 7, e42444.
- 753 Task Team 2015. Recommended phosphorus loading targets for Lake Erie. Annex 4 Objectives
754 and Targets Task Team Final Report to the Nutrients Annex Subcommittee. May 2015.
755 <http://tinyurl.com/pevwt8g>.
- 756 Tomlinson, L., Auer, M., Bootsma, H., 2010. The Great Lakes Cladophora Model: Development
757 and application to Lake Michigan. *J. Great Lakes Res.* 36, 287–297.
- 758 Valipour, R., Leon, L., Depew, D., Dove, A., Rao, Y., n.d. High-resolution modeling for
759 development of nearshore ecosystem objectives in eastern Lake Erie. *J. Gt. Lakes Res.* This
760 issue.
- 761 Vallentyne, J.R., Thomas, N.A., 1978. Fifth Year Review of Canada-United State Great Lakes
762 Water Quality Agreement. Report of Task Group III. A Technical Group to Review
763 Phosphorus Loadings.
- 764 Vanderploeg, H.A., Liebig, J.R., Carmichael, W.W., Agy, M.A., Johengen, T.H., Fahnenstiel,
765 G.L., Nalepa, T.F., 2001. Zebra mussel (*Dreissena polymorpha*) selective filtration
766 promoted toxic *Microcystis* blooms in Saginaw Bay (Lake Huron) and Lake Erie. *Can. J.*
767 *Fish. Aquat. Sci.* 58, 1208–1221.
- 768 Verhamme, E., Redder, T., Schlea, D., Grush, J., Bratton, J., DePinto, J., n.d. Development of
769 the Western Lake Erie Ecosystem Model (WLEEM): application to connect phosphorus
770 loads to cyanobacteria biomass. *J. Gt. Lakes Res.* This issue.
- 771 Vollenweider, R., 1976. Advances in defining critical loading levels for phosphorus in lake
772 eutrophication. *Mem. dell'Istituto Ital. di Idrobiol.* 33, 53–83.
- 773 Weller, D.E., Benham, B., Friedrichs, M., Najjar, R., Paolisso, M., Pascual, P., Shenk, G.,
774 Sellner, K., 2013. Multiple Models for Management in the Chesapeake Bay. STAC
775 Publication Number 14-004, Edgewater, MD.
- 776 Young, T.C., Depinto, J. V, Martin, S.C., Bonner, J.S., 1985. Algal-Available Particulate
777 Phosphorus in the Great Lakes Basin. *J. Great Lakes Res.* 11, 434–446.
- 778 Zhang, H., Culver, D. a., Boegman, L., 2008. A two-dimensional ecological model of Lake Erie:
779 Application to estimate dreissenid impacts on large lake plankton populations. *Ecol.*
780 *Modell.* 214, 219–241. doi:10.1016/j.ecolmodel.2008.02.005
- 781 Zhang, H., Culver, D., Boegman, L., 2011. Dreissenids in Lake Erie: an algal filter or a
782 fertilizer? *Aquat. Invasions* 6, 175–194.

- 783 Zhang, H., Culver, D., Boegman, L., n.d. Spatial distributions of external and internal
784 phosphorus loads and their impacts on Lake Erie's phytoplankton. *J. Gt. Lakes Res.* This
785 issue.
- 786 Zhou, Y., Obenour, D.R., Scavia, D., Johengen, T.H., Michalak, A.M., 2013. Spatial and
787 temporal trends in Lake Erie hypoxia, 1987-2007. *Environ. Sci. Technol.* 47, 899–905.
788 doi:10.1021/es303401b
- 789

Figure Captions

Figure 1. Annual average TP and DRP loads delivered to the Western Basin by major tributaries (upper panel), and annual average flow (lower left panel) and flow weighted mean TP concentration (FWMC, lower right panel) from the same tributaries.

Figure 2. WB cyanobacteria bloom size predicted by three different models as a function of spring Maumee River TP load: a) NOAA Western Lake Erie HAB model; b) U-M/GLERL Western Lake Erie HAB model; c) Western Lake Erie Ecosystem Model (WLEEM). Solid lines are mean model predictions, while dashed lines and shaded area represent 95% predictive intervals. In a), 70% predictive intervals are also shown as reported in Stumpf et al. (this issue). In b), model predictions under 2008 (grey) and 2014 (black) lake conditions are shown. Because the models consider different spring load periods (see text), Maumee River load is reported as MT/month to facilitate comparison across models. The horizontal line indicates the threshold for “severe” blooms, which equals 9600 MT for the first two models and was adjusted to an equivalent of 7830 MT for the WLEEM model (see text and Verhamme et al., this issue). The corresponding March-July cumulative loads are reported in Table 2.

Figure 3. Average summer chlorophyll-*a* concentration in the WB predicted by different models as a function of annual WB TP loads. Each response curve has been scaled to 100% at its maximum chlorophyll value to facilitate comparisons. The dashed line represents a 40% reduction from the 2008 WB annual load.

Figure 4. CB hypoxia metrics predicted by different models as a function of WB + CB annual TP load: a) August-September average hypolimnetic DO concentration in the CB. The horizontal line represents the average concentration (4 mg/L) corresponding to initiation of statistically significant hypoxic areas (Zhou et al., 2013); b) August-September average extent of the CB

hypoxic area. The horizontal line indicates a threshold of 2000 km²; c) Number of hypoxic days in the CB. The shaded area indicates the range of loads required to achieve the hypoxic area threshold of 2000 km². Results for the EcoLE model are shown considering a bottom layer of 1 m (EcoLE_1m) and 1-3 m (EcoLE_1-3m). Results for the 1-D hypoxia model are shown considering a constant net apparent TP deposition rate in the WB (1D Hypoxia_WBconst) and considering TP loads from the WB to the CB as simulated by the WLEEM model (1D Hypoxia_WLEEM).

Figure 5. *Cladophora* biomass predicted by the *Cladophora* Growth Model coupled with the 3-D ELCOM-CAEDYM model in the northern shoreline of the EB as a function of whole lake annual TP load. Load-response curves were developed for two years (2008 and 2013) and at various depth ranges (a-e). For each year and depth range, spatially averaged maximum *Cladophora* biomass and associated 5th and 95th percentiles are shown.

Table 1. Models included in the multi-model effort and Ecosystem Response Indicators (ERIs) addressed by each.

	Ecosystem Response Indicators			
	Basin-specific overall phytoplankton biomass	WB cyanobacteria peak summer biomass	CB hypoxia	EB <i>Cladophora</i>
NOAA Western Lake Erie HAB Model		X		
U-M/GLERL Western Lake Erie HAB Model		X		
Total Phosphorus Mass Balance Model	X			
1-D Central Basin Hypoxia Model	X (CB only)		X	
Ecological Model of Lake Erie (EcoLE)	X (WB only)		X	
Nine-Box Model			X	
Western Lake Erie Ecosystem Model (WLEEM)	X (WB only)	X		
ELCOM-CAEDYM	X		X	X
Great Lakes <i>Cladophora</i> Model (GLCM)				X

Table 2. TP loads (MT) associated with example ERI thresholds. Annual Maumee River TP loads corresponding to the suggested March - July loads were calculated assuming the March-July load represents on average 53% of the annual load (data from Heidelberg University's National Center for Water Quality Research, <http://tinyurl.com/zgkberb>). The corresponding WB annual loads were calculated assuming the Maumee annual load represents on average 48% of the whole WB annual load (Maccoux et al., this issue). The whole lake annual loads corresponding to the suggested hypoxia-related WB+CB loads were calculated assuming the WB+CB load represents on average 88% of the whole lake load (Maccoux et al., this issue).

Model	Maumee March-July load to achieve threshold	Maumee annual load to achieve threshold	WB annual load to achieve threshold	WB + CB annual load to achieve threshold	Whole lake annual load to achieve threshold
Loads to reduce Western Basin Cyanobacteria to 9600 MT cell DW					
UM/GLERL_2008	1150	2170	4520		
NOAA	900	1698	3538		
WLEEM	890	1679	3498		
Mean ± St. Dev.	980 ±147 *	1849 ± 278*	3852 ± 579*	*using UM/GLERL_2008	
Loads to reduce Central Basin Hypolimnetic Dissolved Oxygen to 4 mg/l					
EcoLE_1-3m				4400	5000
EcoLE_1m				2600	2955
ELCOM-CAEDYM				3100	3523
1D CB Hypoxia_WBconst				5100	5795
1D CB Hypoxia_WLEEM				4000	4545
Mean ± St. Dev.				3840 ±1001	4364 ±1138
Loads to reduce Central Basin Hypoxic Area to 2000 km²					
EcoLE_1-3m				5955	6767
EcoLE_1m				3415	3881
ELCOM-CAEDYM				4920	5591
1D CB Hypoxia_WBconst				4830	5489
1D CB Hypoxia_WLEEM				3880	4409
Mean ± St. Dev.			*omitting 9=Box	4600 ± 989*	5227 ± 1124*
Loads to reduce <i>Cladophora</i> dry weight biomass to 30 g/m²					
GLCM/ELCOM-CAEDYM					See Text

Figure 1. Annual average TP and DRP loads delivered to the Western Basin by major tributaries (upper panel), and annual average flow (lower left panel) and flow weighted mean TP concentration (FWMC, lower right panel) from the same tributaries.

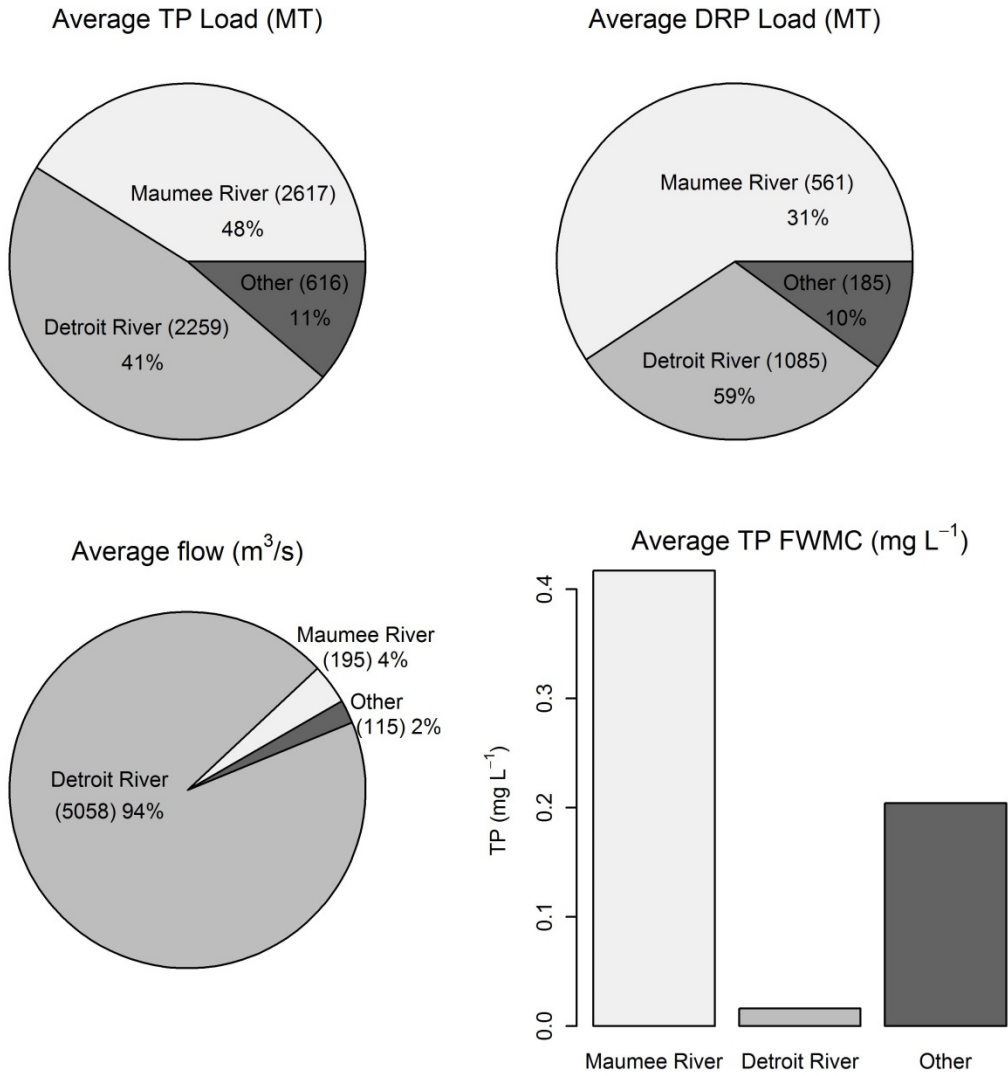


Figure 2. WB cyanobacteria bloom size predicted by three different models as a function of spring Maumee River TP load: a) NOAA Western Lake Erie HAB model; b) U-M/GLERL Western Lake Erie HAB model; c) Western Lake Erie Ecosystem Model (WLEEM). Solid lines are mean model predictions, while dashed lines and shaded area represent 95% predictive intervals. In a), 70% predictive intervals are also shown as reported in Stumpf et al. (this issue). In b), model predictions under 2008 (grey) and 2014 (black) lake conditions are shown. Because the models consider different spring load periods (see text), Maumee River load is reported as MT/month to facilitate comparison across models. The horizontal line indicates the threshold for “severe” blooms, which equals 9600 MT for the first two models and was adjusted to an equivalent of 7830 MT for the WLEEM model (see text and Verhamme et al., this issue). The corresponding March-July cumulative loads are reported in Table 2.

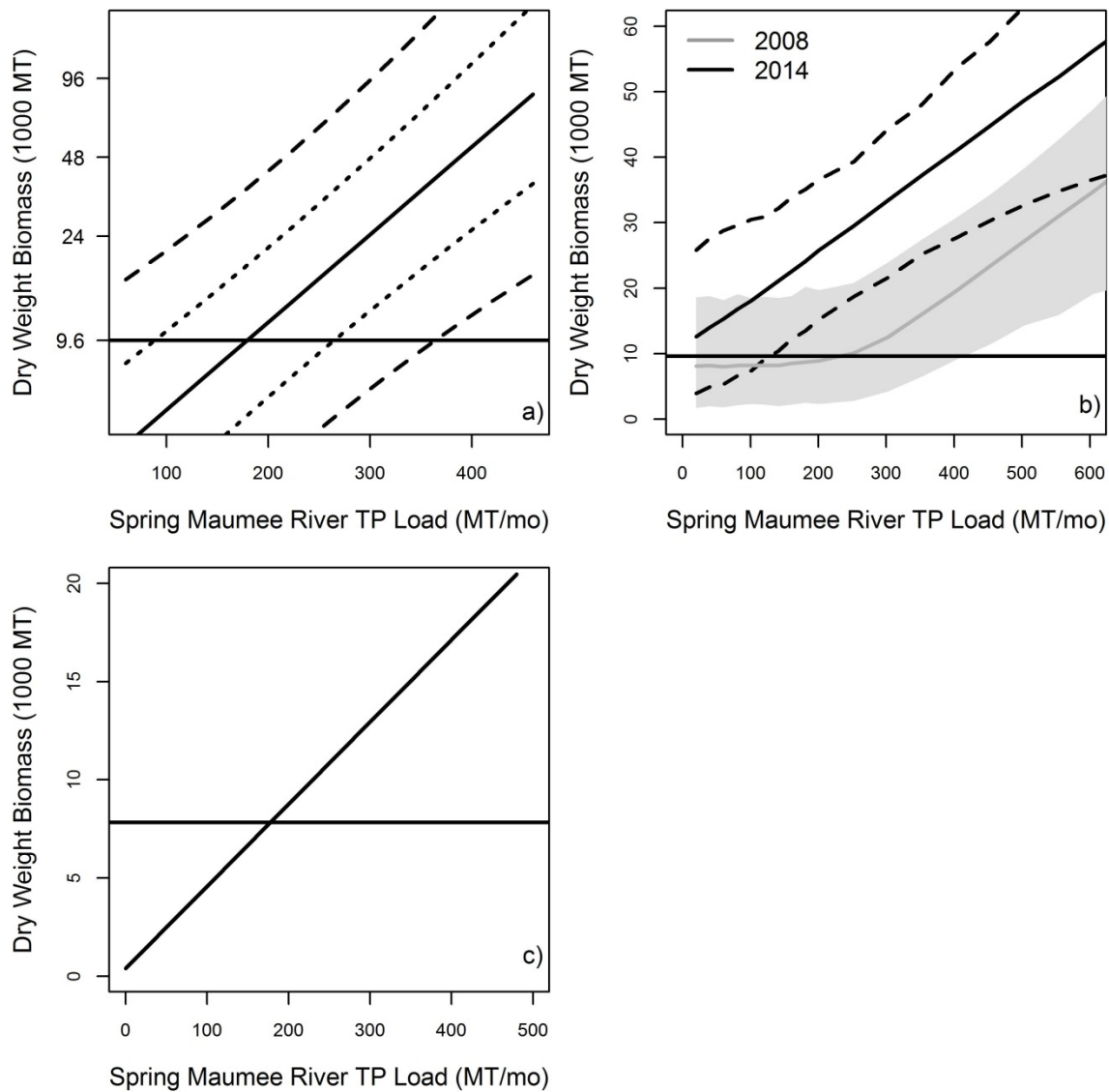


Figure 3. Average summer chlorophyll-*a* concentration in the WB predicted by different models as a function of annual WB TP loads. Each response curve has been scaled to 100% at its maximum chlorophyll value to facilitate comparisons. The dashed line represents a 40% reduction from the 2008 WB annual load.

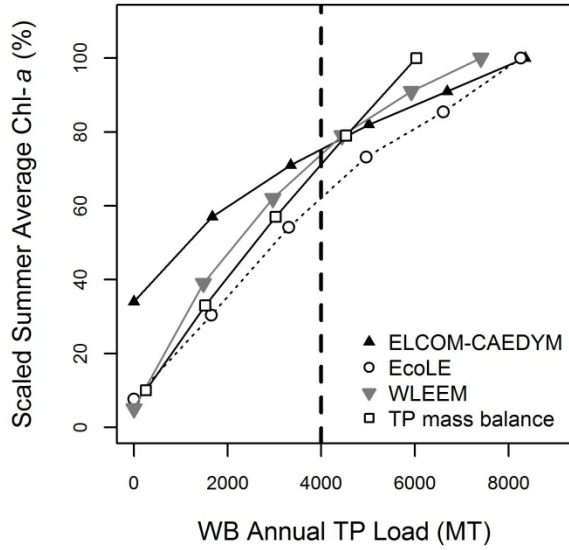


Figure 4. CB hypoxia metrics predicted by different models as a function of WB + CB annual TP load: a) August-September average hypolimnetic DO concentration in the CB. The horizontal line represents the average concentration (4 mg/L) corresponding to initiation of statistically significant hypoxic areas (Zhou et al., 2013); b) August-September average extent of the CB hypoxic area. The horizontal line indicates a threshold of 2000 km²; c) Number of hypoxic days in the CB. The shaded area indicates the range of loads required to achieve the hypoxic area threshold of 2000 km². Results for the EcoLE model are shown considering a bottom layer of 1 m (EcoLE_1m) and 1-3 m (EcoLE_1-3m). Results for the 1-D hypoxia model are shown considering a constant net apparent TP deposition rate in the WB (1D Hypoxia_WBconst) and considering TP loads from the WB to the CB as simulated by the WLEEM model (1D Hypoxia_WLEEM).

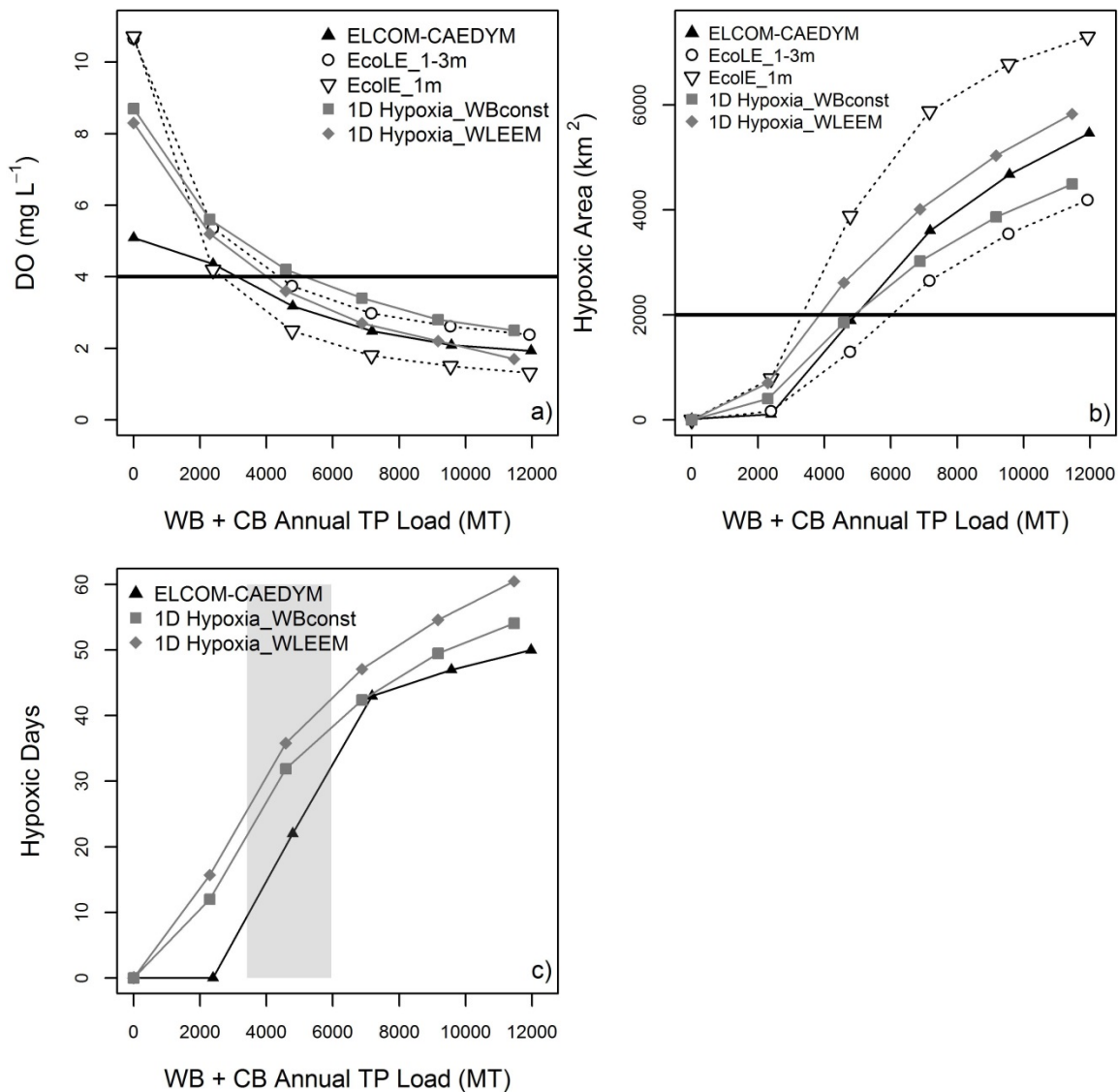


Figure 5. *Cladophora* biomass predicted by the *Cladophora* Growth Model coupled with the 3-D ELCOM-CAEDYM model in the northern shoreline of the EB as a function of whole lake annual TP load. Load-response curves were developed for two years (2008 and 2013) and at various depth ranges (a-e). For each year and depth range, spatially averaged maximum *Cladophora* biomass and associated 5th and 95th percentiles are shown.

